Improvement of NbOx-based threshold switching devices by implementing multilayer stacks

Semiconductor Science and Technology

PAPER • **OPEN ACCESS**

Improvement of NbO_x-based threshold switching devices by implementing multilayer stacks

To cite this article: Melanie Herzig *et al* 2019 *Semicond. Sci. Technol.* **34** 075005

OPEN ACCESS
IOP Publishing
Semiconductor Science and Technology
Semicond. Sci. Technol. **34** (2019) 075005 (7pp)
https://doi.org/10.1088/1361-6641/ab1da3

Improvement of NbO_x-based threshold switching devices by implementing multilayer stacks

Melanie Herzig[1,4], **Martin Weiher**[2], **Alon Ascoli**[2], **Ronald Tetzlaff**[2], **Thomas Mikolajick**[1,3] **and Stefan Slesazeck**[1]

[1] NaMLab gGmbH, Noethnitzer Str. 64, Dresden D-01187, Germany
[2] Faculty of Electrical and Computer Engineering, Technische Universitaet Dresden, D-01062 Dresden, Germany
[3] Chair of Nanoelectronic Materials, Technische Universitaet Dresden, D-01187 Dresden, Germany

E-mail: melanie.herzig@namlab.com, martin.weiher@tu-dresden.de, alon.ascoli@tu-dresden.de, ronald.tetzlaff@tu-dresden.de, thomas.mikolajick@namlab.com and stefan.slesazeck@namlab.com

Received 22 January 2019, revised 27 March 2019
Accepted for publication 29 April 2019
Published 6 June 2019

Abstract

In this work the *I–V* characteristics of a niobium oxide-based threshold switching device were optimized to match the requirements for its application in neuromorphic circuits. Those neuromorphic circuits rely on coupled oscillators utilizing the volatile resistive switching effect of the memristor. A large voltage extension of the negative differential resistance region of the threshold switch enables enhanced signal amplification, and, furthermore, can lead to a better tolerance to device variability. A symmetric switching behavior as well as a high device stability for the operation in both voltage polarities is mandatory to allow the integration in circuits that utilize the connection of several threshold switching devices operated in different polarities. These properties are similarly important for the adoption of the threshold switches as selector devices in bipolar resistive memory arrays. Furthermore, a low forming voltage is desirable because it leads to a better control during the forming step. To meet all those requirements the application of multilayer stacks consisting of niobium and niobium oxide layers is proposed and their optimization is investigated in detail.

Keywords: threshold switching, memristor, neuromorphic, oscillator, selector device

(Some figures may appear in colour only in the online journal)

1. Introduction

Threshold switching in niobium oxide-based devices has already been known for a long time [1]. This threshold switching manifests itself as a hysteresis loop in the *I–V* characteristics. It originates from a negative differential resistance (NDR) region that can be stabilized by either connecting a large enough resistor (whose resistance is at least sufficiently large to compensate the NDR) in series to the device or by performing a current sweep [2]. A now widely accepted explanation for the threshold switching effect in niobium oxide is a temperature-activated Frenkel–Poole conduction [2–7]. Already in one of the first publications dealing with threshold switching in niobium oxide, the feasibility of a relaxation oscillator circuit based on those devices was demonstrated and recently, the dynamics of such a circuit were investigated in more detail [8, 9]. In the last few years this topic was revived using modern semiconductor technology and the knowledge obtained from RRAM research

[4] Author to whom any correspondence should be addressed

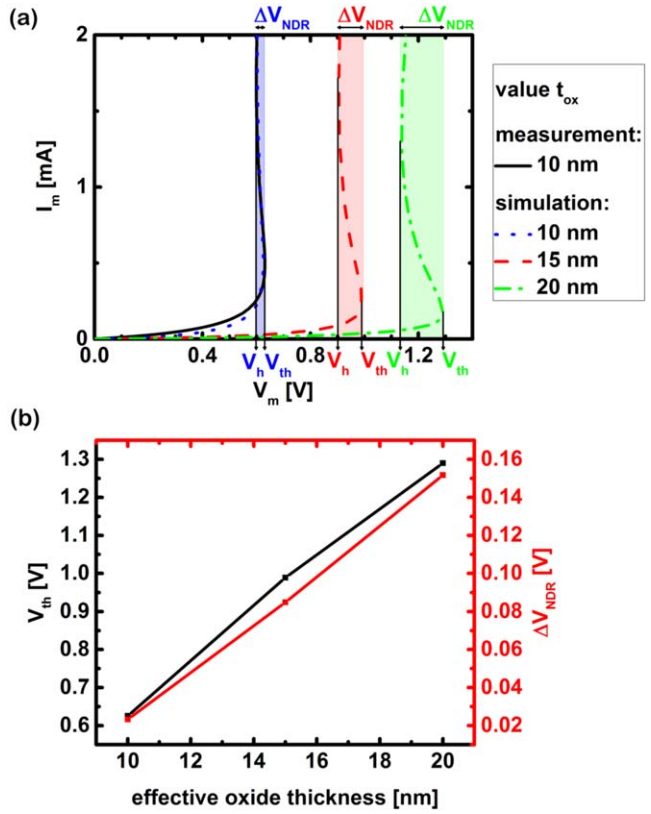

Figure 1. (a) Measured (solid, black) and simulated (dotted, blue) current–voltage characteristic of a bi-layer sample consisting of a 10 ± 0.2 nm niobium oxide top layer and a 4.5 ± 0.1 nm niobium bottom layer together with simulations for t_{ox} equal to 15 nm (dashed, red) and 20 nm (dotted–dashed, green). The voltage extension of the NDR region is visualized by colored regions. I_m denotes the current through the threshold switch, while V_m is the voltage across it. For each value of t_{ox} the hold voltage V_h, identifying the end of the NDR region, is also highlighted. b) Values of V_{th} and ΔV_{NDR} extracted from the simulation results depicted in figure 1(a) for different effective oxide thicknesses.

[10, 11] as well as from memristor theory [12]. Furthermore, in 2012 it was successfully demonstrated that it is possible to build a neuristor circuit using threshold switching-based oscillators [13]. For these and similar applications, it is necessary to optimize the threshold switching devices to achieve a symmetric behavior for both voltage polarities because this enables a considerably simpler design of circuits like the neuristor circuit in [13], where devices have to be operated in different polarities. Additionally a large voltage extension of the NDR region is mandatory since it directly influences the amplitude of the output signal and therefore determines if a transmission via several stages with threshold switching devices is possible. A large voltage extension of the NDR region may also lead to a better tolerance to device variability. Furthermore, a low forming voltage is beneficial because a too large forming voltage can have a negative influence on the variability of threshold voltage and threshold current of the threshold switches [14] and makes the array integration more complicated [15]. Another possible field of application is the combination of a niobium oxide-based threshold switch acting as a selector element with a non-volatile resistive switch [15–21]. For this type of application, a symmetric switching behavior for both voltage polarities is the most important feature if a combination with a bipolar resistive switch shall be implemented.

2. Experimental

Our threshold switching devices consist of a niobium–niobium oxide bi-layer stack or a niobium oxide-niobium–niobium oxide three-layer stack sandwiched between two platinum electrodes. As top electrodes, evaporated platinum dots with a diameter of 50 μm were used. The niobium and niobium oxide layers were both sputtered from a niobium target. The niobium oxide layer was reactively sputtered with 26.7% oxygen added to the argon atmosphere. The measurements of the quasi-static *I–V* characteristics of those samples were carried out using current sweeps, whereas the forming voltage was determined within a voltage sweep utilizing a Keithley 4200 A semiconductor parameter analyzer. During those measurements the bottom electrode was grounded and a certain voltage was applied to the top electrode.

3. Results and discussion

To achieve threshold switching in niobium oxide-based devices, a stack consisting of a layer with a low oxygen content in combination with a layer with a high oxygen content can be used [22, 23]. The resulting threshold switching effect can be explained as the result of a temperature-activated Frenkel–Poole conduction phenomenon [2]. This conduction mechanism can be described by a temperature- and voltage-dependent Ohm's law, where the memristance R is expressed by

$$R(V_m, T) = R_0 \cdot \mathrm{e}^{\frac{E_a - \frac{q^2 N_D^{1/3}}{4\pi\varepsilon_0\varepsilon_r} - \frac{q\cdot\lambda}{t_{ox}}\cdot V_m}{kT}}. \quad (1)$$

V_m stands for the voltage across the threshold switching device, while the resistance R_0 is given by

$$R_0 = \frac{4t_{ox}}{N_c \mu q \pi {d_{fil}}^2}, \quad (2)$$

with the activation energy E_a and the donor state concentration N_D. λ is a fitting parameter, which expresses the decentering of the maximum of the potential well between two donor states due to the impact of the electric field, q denotes the elementary charge, t_{ox} the effective oxide thickness, ε_0 and ε_r represent the vacuum and relative permittivity respectively, while k refers to the Boltzmann constant. The resistance R_0 depends on the effective oxide thickness t_{ox}, the density of states N_C in the conduction band, the electron mobility μ and the filament diameter d_{fil}. The temperature T inside the filament depends on its heating by

Table 1. Fitting parameter list used to obtain the curves in figure 1.

Parameter	Value	Unit
E_a	0.215	eV
q	1.602×10^{-19}	C
N_D	5.959×10^{20}	cm^{-3}
λ		nm
t_{ox}	10 (15, 20)	nm
ε_0	8.85×10^{-12}	$F\,m^{-1}$
ε_r	20	
k	8.617×10^{-5}	$eV\,K^{-1}$
Γ_{th}	2×10^{-6}	$W\,K^{-1}$
N_c	5.6×10^{19}	cm^{-3}
μ	0.003	$cm^2\,V^{-1}\,s^{-1}$
d_{fil}	83.26	nm

Joule effect. The rate of change of T, i.e. $\dot{T}$: $=dT/dt$, can be expressed by

$$C_{th}\dot{T} = \frac{{V_m}^2}{R} - \Gamma_{th}\Delta T. \quad (3)$$

Apart from the influence of the temperature difference ΔT between the ambient temperature and the temperature inside the filament, $\dot{T}$ also depends upon the thermal capacitance C_{th} as well as on the thermal conductance Γ_{th}. C_{th} has no influence on the experimental quasi-static current–voltage characteristics since in the respective measurements $\dot{T} = 0$. However, this parameter has a crucial impact on the dynamic behavior of the device. In figure 1 the quasi-static current–voltage characteristic of a sample consisting of a bi-layer stack, composed of a 10 ± 0.2 nm thick niobium oxide (NbO_x) top layer and a 4.5 ± 0.1 nm thick niobium (Nb) bottom layer, is shown. There is a good agreement between the simulation model (dotted blue curve) and the measurement (solid black curve). The values of the physical constants used in this simulation are given in table 1. As a simplification, it was assumed that the effective oxide thickness equals the thickness of the deposited NbO_x layer. This assumption is based on the presumption that no reaction at the interface between Nb and NbO_x takes place. As a result the effective oxide thickness is therefore neither reduced nor increased. Most likely this introduces a certain inaccuracy in modeling the quantitative behavior of the stack, but our mathematical description captures rather well its qualitative behavior.

Inside the filament a very large donor state concentration N_D was obtained while the fit provided a small relative permittivity ε_r. The obtained values suggest that, after the electroforming step is completed, the filament contains a lot of oxygen vacancies, which act as donor states, going hand in hand with a decrease in the relative permittivity [24]. Although, the fit results point on a high donor state concentration in the filament, whereas the dielectric constant is smaller than the one of stochiometric Nb_2O_5, those values do not represent absolute results, since a variation in ε_r could be compensated by changing N_D accordingly. Note that none of the two parameters could be experimentally determined independently from the fitting procedure. Using a sample, which is comparable to the measured one, in an oscillator-based application has the disadvantage that the experimentally determined average voltage extension of the NDR region ($\overline{\Delta V_{NDR}}$), which was determined based on 30 measurements, is smaller than 50 mV. This voltage extension of the NDR region is defined as the difference between the threshold voltage (V_{th}), after which the I_m–V_m characteristic features a negative slope, and the hold voltage (V_h), after which the slope of the I_m–V_m characteristic turns positive once again. An increase in the voltage extension of the NDR region could be achieved by changing any of the parameters [25] in equations (1)–(3) except C_{th}. However, not all of the parameters can be easily influenced by means of changes in the processing of the sample stack. One parameter that can be easily adjusted, is the effective oxide thickness t_{ox}, because it is directly related to the thickness of the deposited niobium oxide top layer. If the effective oxide thickness is increased in equations (1) and (2), assuming that all the other parameters remain constant, numerical simulations of the proposed model reveal the emergence of a larger voltage extension of the NDR region, caused by a reduction of the slope in the I_m–V_m characteristics in the NDR region itself (see figure 1(a)). According to these simulations, doubling the effective oxide thickness from 10 to 20 nm should lead to a significant approximately linear increase in the voltage extension of the NDR region, which is accompanied by a concurrent increase in the threshold voltage (see figure 1(b)).

In order to verify this observation, the I_m–V_m characteristics of 30 devices respectively for samples with 10 ± 0.2, 15 ± 0.3, and 20 ± 0.4 nm thickness of the niobium oxide top layer were measured and statistically evaluated. The schematic of the three different sample stacks is depicted in figure 2(a). From figure 2(b) it is evident that the average voltage extension of the NDR region ($\overline{\Delta V_{NDR}}$) indeed increases when the NbO_x layer thickness is increased. The measured increase is smaller than expected from the simulation results (represented by the red dots in figure 2(b)). This might be caused by a deviation between the thickness of the deposited oxide layer and the effective oxide thickness t_{ox}, which might result from a reaction between the niobium oxide layer and the subjacent niobium layer or by a concurrent change in other parameters, e.g. Γ_{th}, N_D and N_C. As expected from the simulation results, the increase in the average voltage extension of the NDR region goes hand in hand with an increase in the average threshold voltage $\overline{V_{th}}$ (see figure 2(c)). This increase is significantly smaller than one would have expected on the basis of the numerical simulation results. As mentioned earlier this may be due to concurrent chage in other device parameters.

A drawback of the increase in the NbO_x top layer thickness is an increase in the forming voltage from an average value of 1.8–3 V. An increase in the forming voltage impairs the reproducibility of the forming process, and leads to a larger variability in the threshold switching parameters (see figures 2(b) and (c)), where the spread in ΔV_{NDR} and V_{th} is the largest for the case of the 20 ± 0.4 nm thick NbO_x layer).

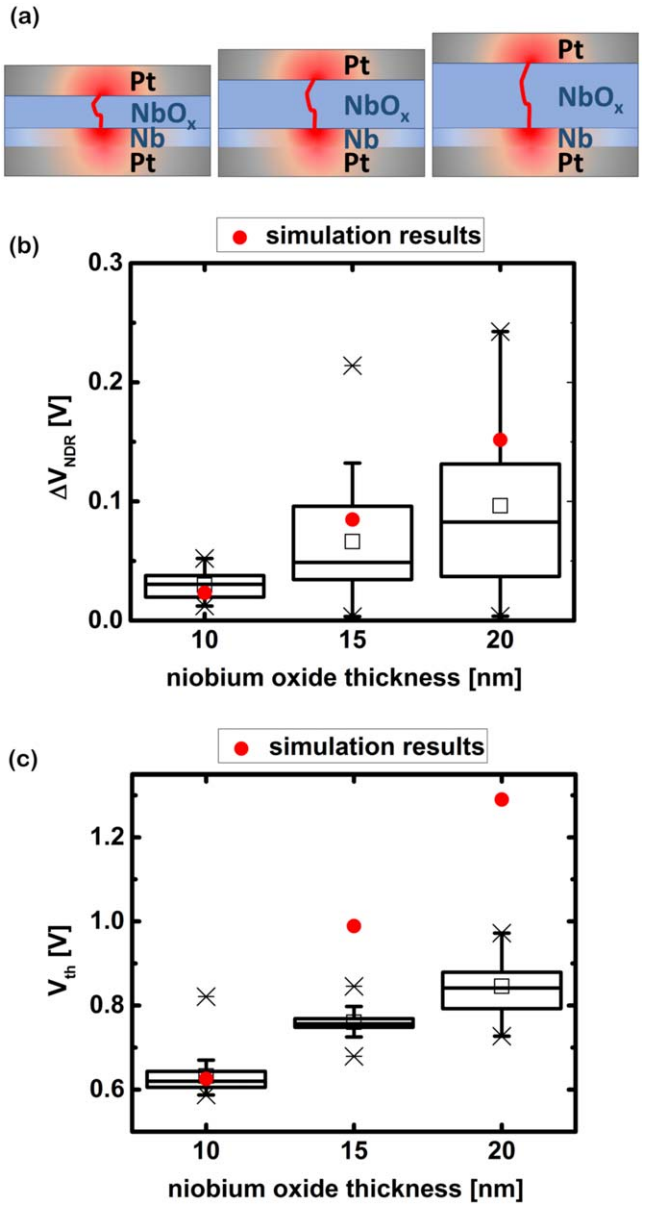

Figure 2. (a) Schematic of the three different sample stacks under investigation. Boxplots showing the distribution of (b) the voltage extension of the NDR region and of (c) the threshold voltage of the three samples with different NbO_x top layer thicknesses for 30 measurements, respectively. The red dots in figures 2(b) and (c) represent the simulation results depicted in figure 1(b).

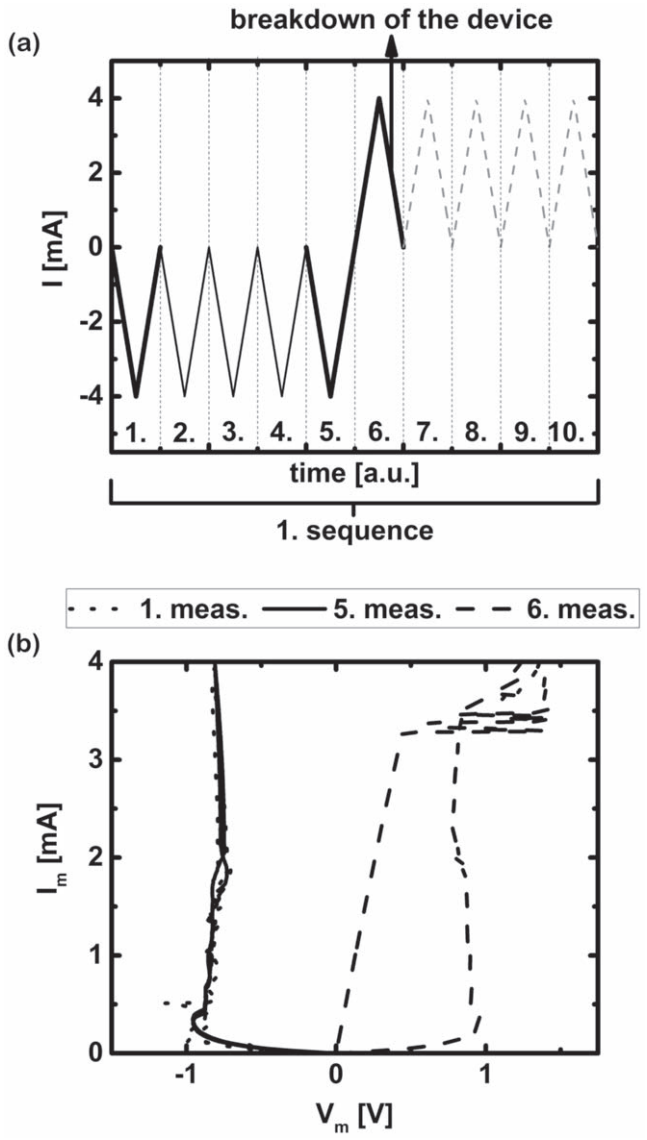

Figure 3. (a) Time-dependent current profile for the first measurement sequence consisting of five consecutive measurements with negative current polarity followed by five consecutive measurements with positive current polarity. b) I_m–V_m characteristics resulting from the first, the fifth, and the sixth measurement of the first measurement sequence (highlighted by thicker lines in figure 3(a)). The measured sample consists of a 20 ± 0.4 nm thick niobium oxide top layer and a 4.5 ± 0.1 nm thick niobium bottom layer.

Besides the need for a large voltage extension of the NDR region, a further requirement to enable an easy application of these devices in neuromorphic circuits like e.g. the neuristors in [13] or as a selector device in bipolar resistive memory arrays, is a symmetric threshold switching behavior for both voltage polarities. In order to investigate whether our devices with a 20 ± 0.4 nm thick niobium oxide top layer and a 4.5 ± 0.1 nm thick niobium bottom layer exhibit such a symmetric threshold switching behavior, they were analyzed using a measurement sequence consisting of five consecutive current sweeps with negative polarity followed by five consecutive current sweeps with positive polarity (see figure 3(a)). Figure 3(b) displays the first, fifth and sixth measurement belonging to the first measurement sequence. It can be observed that the threshold characteristic stabilizes in the first measurement sequence during the negative current phase. On the contrary, the subsequent application of a current sweep with positive polarity reveals instabilities in the device, which switches to a different resistance state, losing the desired threshold switching behavior. This unwanted phenomenon can be attributed to the asymmetric device stack. Therefore, in order to achieve an enhanced symmetry, the device structure was changed from a bi-layer to a three-layer stack, which resembels the device configuration used in complementary resistive switches [26]. This was realized by introducing an additional niobium oxide layer below the

metallic niobium layer. Multilayer stacks comprising niobium oxide layers were already succesfully applied in the past to meet the requirements of different applications [19–21, 27, 28]. Forthe samples consisting of a three-layer stack the thicknesses of the top NbO_x and the middle Nb layers were kept constant at 10 ± 0.2 nm and 4.5 ± 0.1 nm, respectively. Assuming that these three-layered threshold switches can still be described via equations (1)–(3) an increase in the thickness of the additional niobium oxide bottom layer should lead to an increase in the effective oxide thickness t_{ox} and eventually in an increase in the voltage extension of the NDR region, and to a concurrent increase in the threshold voltage, comparable to the phenomena observed with the increase in the niobium oxide top layer thickness in the bi-layer stack. This expectation is confirmed in the statistical evaluation of 30 measured I_m–V_m characteristics for samples with 0 nm, 2.5 ± 0.1 nm, 5 ± 0.1 nm, 7.5 ± 0.2 nm and 10 ± 0.2 nm thickness of the niobium oxide bottom layer (see schematic in figure 4(a)), respectively. In order to achieve a threshold switching behavior of similar nature as the one observed for bi-layer stacks, a two-step forming process, consisting of the application of current sweeps with both polarities, had to be performed on the three-layer samples with a niobium oxide bottom layer thickness equal to or larger than 5 ± 0.1 nm. This was most likely necessary for the formation of a strong filament through both niobium oxide layers. For the samples, for which a two-step forming process was necessary, the voltage extension of the NDR region was evaluated on the basis of the current–voltage characteristics measured with a positive current polarity. The investigation based on figure 4(b) revealed that the median value of the voltage extension of the NDR region increases from 30 mV without an additional niobium oxide bottom layer to 153 mV with an additional 10 ± 0.2 nm thick niobium oxide bottom layer. This high median value of ΔV_{NDR} is even larger than the median value of 100 mV that was achieved for the bi-layered sample with a 20 ± 0.4 nm thick niobium oxide top layer. The observed increase in the median value of the voltage extension of the NDR region approximately follows the trend that was expected based upon the simulation results reported in figure 1, which are marked in figure 4(b) through the use of red dot symbols. The high median value of 153 mV for the voltage extension of the NDR region, observed in the stack with a 10 ± 0.2 nm thick NbO_x bottom layer, could be attributed to an increase in the effective oxide thickness caused by the partial oxidation of the niobium middle layer at both interfaces with the oxide layers (whereas, in the bi-layer structure the Nb bottom layer may undergo oxidation at the top interface only).

Furthermore, this large value could be caused by a change in the donor state concentration, resulting from the application of a voltage with positive polarity, which may be accompanied by the emergence of a small non-volatile resistive switching effect [22, 29]. Both conjectures, based either on an increased effective oxide thickness due to the oxidation of the niobium layer or on an increased donor state concentration caused by the variation in the measurement procedure, which is necessary as the thickness of the bottom oxide layer is increased, would also explain the significantly

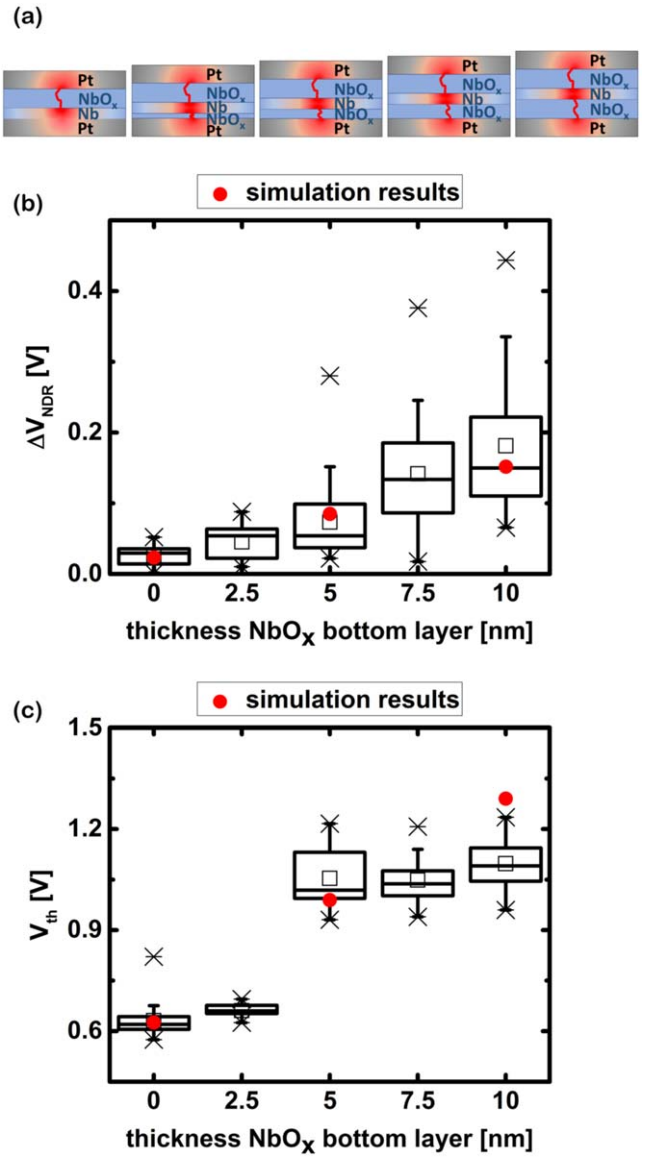

Figure 4. (a) Schematic of the five different sample stacks under investigation. Boxplots showing the distribution of (b) the voltage extension of the NDR region and (c) the threshold voltage of the five samples with different NbO_x bottom layer thicknesses for 30 measurements, respectively. The red dots in figures 4(b) and (c) represent the simulation results depicted in figure 1(b).

increased threshold voltage, which is observed in figure 4(c) as soon as the thickness of the NbO_x bottom layer is increased from only 2.5 ± 0.1 to 5 ± 0.1 nm. A further advantage of the three-layer stack with two 10 ± 0.2 nm thick niobium oxide layers, besides the increase in the voltage extension of the NDR region, is the decrease in the voltage necessary for a proper electroforming. The median was found to be 2.4 V, which is considerably lower than the median forming voltage of 3 V necessary for a bi-layer stack with a 20 ± 0.4 nm thick niobium oxide top layer. This significant decrease in the median forming voltage provides the advantage of a reduction in the necessary supply voltage (and thus in the power consumption) during the initial forming step. Further, it allows to realize the forming process directly inside an integrated

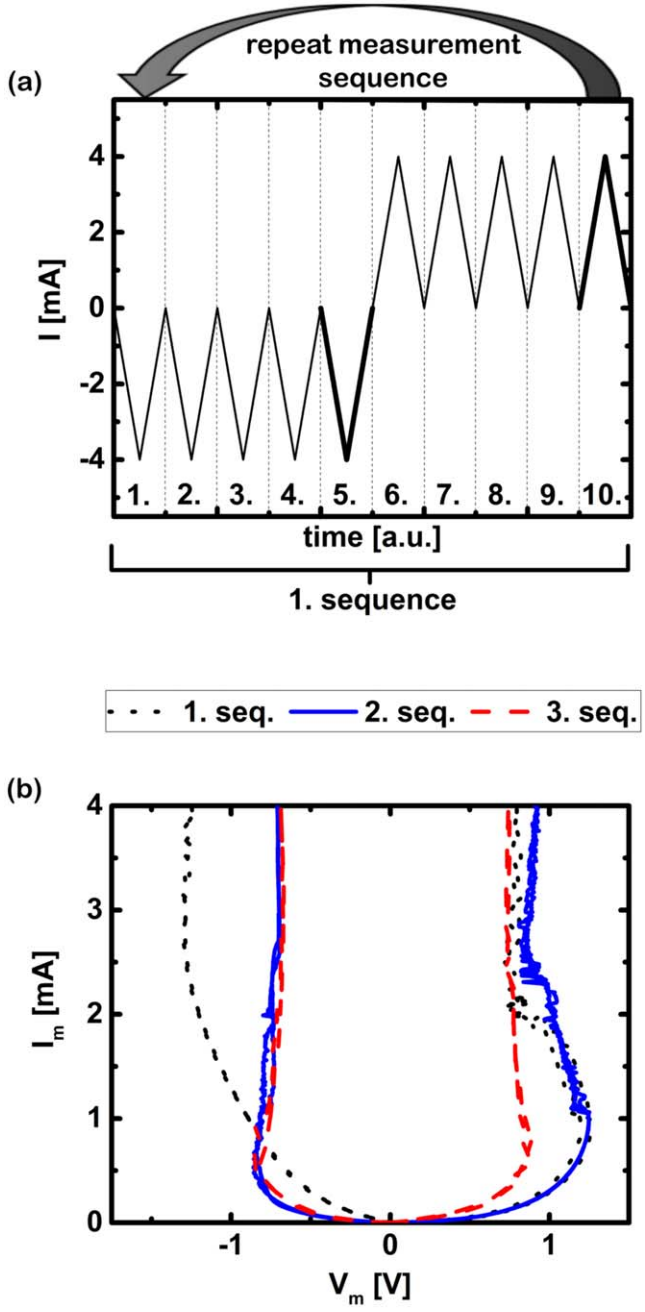

Figure 5. (a) Time-dependent current profile for the first measurement sequence consisting of five consecutive measurements with negative current polarity followed by five consecutive measurements with positive current polarity. (b) I_m-V_m characteristics of the fifth and tenth measurement (highlighted by thicker lines in figure 5(a)) within each of the first three consecutive measurement sequences of the kind depicted in plot (a). The measured sample consists of a 4.5 ± 0.1 nm thick niobium layer sandwiched between two 10 ± 0.2 nm thick niobium oxide layers.

circuit incluing other components characteriszed by a sensitivity to large voltages, such as select transistors or additional resistive switching devices adopted to adjust synaptic weights during learning processes [10, 30]. Furthermore, the three-layer stack with a 10 ± 0.2 nm thick NbO_x bottom layer shows the desired improved symmetry in the threshold switching behavior, as shown in figure 5(b). As was already mentioned earlier in the discussion of the forming step, for samples with a three-layer stack, including two relatively thick niobium oxide layers, a good threshold switching performance is only achievable after the application of current sweeps with both polarities. Therefore, with reference to figure 5, the first five measurements with a negative current polarity revealed only a weak threshold switching performance with a small voltage extension of the NDR region. The consecutive application of sweeps with a positive current led to an increase in the voltage extension of the NDR region, and to a stable switching behavior of the device, which, in fact, was observed without major changes after reversing the voltage polarity in the second measurement sequence. More in detail, repeating the first measurement sequence two more times led to the emergence of reproducible threshold switching characteristics and over the course of the measurement routine, the current–voltage characteristics became more and more symmetric. Within the five measurements per current polarity in the third measurement sequence, no significant variation was observed in the respective I_m-V_m characteristics, demonstrating that the three-layer threshold switching device under study achieves a stable state for each voltage polarity. Overall the symmetry in the threshold switching behavior of the three-layer sample stack was found to be considerably improved as compared to the bi-layer case. This enables a symmetric operation of the three-layer device after undergoing a few preconditioning measurement cycles. The remaining small symmetry difference might be caused by the slight difference between the top and bottom electrode/oxide-interfaces due to the different adopted deposition techniques and the vacuum break prior to the top electrode deposition.

4. Conclusion

In this work, we demonstrated that the transition from a bi-layer stack, consisting of a NbO_x top layer and a Nb bottom layer, to a three-layer stack, composed of a Nb layer sandwiched between two NbO_x layers, results in an improved performance of the threshold switching devices. With a three-layer stack in place of a bi-layer stack, the voltage extension of the NDR region can be increased thanks to the resulting increase in the effective niobium oxide thickness. Furthermore, the proposed stack endows the device with almost symmetric threshold switching behavior under voltages of opposite polarities. Moreover, the transition to a three-layer stack reduces the voltage necessary during the electroforming step. This allows to have a better control of the overall forming process, resulting in a smaller device-to-device variability. The improved performance of the multilayer stacks simplifies the adoption of threshold switching devices in nonlinear circuits [31], and improves their suitability to act as selector devices in bipolar resistive memory crossbar arrays.

Acknowledgments

The German Research Foundation (Deutsche Forschungsgemeinschaft) is acknowledged for funding this research in the frame of the project 'LAMP' (project no. 273537230 (MI 1247/12-1)).

ORCID iDs

Melanie Herzig https://orcid.org/0000-0002-0681-5441
Stefan Slesazeck https://orcid.org/0000-0002-0414-0321

References

[1] Geppert D V 1963 *Proc. IEEE* **51** 223–223
[2] Slesazeck S, Mähne H, Wylezich H, Wachowiak A, Radhakrishnan J, Ascoli A, Tetzlaff R and Mikolajick T 2015 *RSC Adv.* **5** 102318–22
[3] Funck C, Menzel S, Aslam N, Zhang H, Hardtdegen A, Waser R and Hoffmann-Eifert S 2016 *Adv. Electron. Mater.* **2** 1600169
[4] Gibson G A *et al* 2016 *Appl. Phys. Lett.* **108** 023505
[5] Li S, Liu X, Nandi S K and Elliman R G 2018 *Nanotechnology* **29** 375705
[6] Joshi T, Borisov P and Lederman D 2018 *J. Appl. Phys.* **124** 114502
[7] Wang Z, Kumar S, Nishi Y and Wong H-S P 2018 *Appl. Phys. Lett.* **112** 193503
[8] Liu X, Li S, Nandi S K, Venkatachalam D K and Elliman R G 2016 *J. Appl. Phys.* **120** 124102
[9] Chopra K L 1963 *Proc. IEEE* **51** 941–2
[10] Hong X, Loy D J, Dananjaya P A, Tan F, Ng C and Lew W 2018 *J. Mater. Sci.* **53** 8720–46
[11] Nishi Y, Sasakura H and Kimoto T 2018 *J. Appl. Phys.* **124** 152134
[12] Ascoli A, Slesazeck S, Mahne H, Tetzlaff R and Mikolajick T 2015 *IEEE Trans. Circuits Syst.* I **62** 1165–74
[13] Pickett M D, Medeiros-Ribeiro G and Williams R S 2013 *Nat. Mater.* **12** 114–7
[14] Slesazeck S, Herzig M, Mikolajick T, Ascoli A, Weiher M and Tetzlaff R 2016 *16th Non-Volatile Memory Technology Symp. (NVMTS) ((IEEE) pp 1–5*
[15] Wylezich H, Reinhardt E, Slesazeck S and Mikolajick T 2015 *Semicond. Sci. Technol.* **30** 115014
[16] Kim K M, Zhang J, Graves C, Yang J J, Choi B J, Hwang C S, Li Z and Williams R S 2016 *Nano Lett.* **16** 6724–32
[17] Cha E *et al* 2013 *IEEE Int. Electron Devices Meeting (IEDM)* (Washington, DC: IEEE) pp 1–10
[18] Cha E, Park J, Woo J, Lee D, Prakash A and Hwang H 2016 *Appl. Phys. Lett.* **108** 153502
[19] Nandi S K, Liu X, Venkatachalam D K and Elliman R G 2015 *J. Phys. D: Appl. Phys.* **48** 195105
[20] Kim S G *et al* 2015 *IEEE Int. Electron Devices Meeting (IEDM)* (Washington, DC: IEEE) pp 1–10
[21] Park J, Cha E, Lee D, Lee S, Song J, Park J and Hwang H 2015 *Microelectron. Eng.* **147** 318–20
[22] Mahne H, Wylezich H, Slesazeck S, Mikolajick T, Vesely J, Klemm V and Rafaja D 2013 *2013 5th IEEE Int. Memory Workshop (IMW)* (Monterey, CA: IEEE) pp 174–7
[23] Wang Y, Comes R B, Wolf S A and Lu J 2016 *IEEE J. Electron Devices Society* **4** 11–4
[24] Hoshina T, Sase R, Nishiyama J, Takeda H and Tsurumi T 2018 *J. Ceram. Soc. Japan* **126** 263–8
[25] Funck C, Hoffmann-Eifert S, Lukas S, Waser R and Menzel S 2017 *J. Comput. Electron.* **16** 1175–85
[26] Linn E, Rosezin R, Kügeler C and Waser R 2010 *Nat. Mater.* **9** 403–6
[27] Park J, Hadamek T, Posadas A B, Cha E, Demkov A A and Hwang H 2017 *Sci. Rep.* **7** 4068
[28] Liu X, Sadaf S M, Son M, Shin J, Park J, Lee J, Park S and Hwang H 2011 *Nanotechnology* **22** 475702
[29] Liu X, Md. Sadaf S, Son M, Park J, Shin J, Lee W, Seo K, Lee D and Hwang H 2012 *IEEE Electron Device Lett.* **33** 236–8
[30] Prezioso M, Merrikh-Bayat F, Hoskins B D, Adam G C, Likharev K K and Strukov D B 2015 *Nature* **521** 61–4
[31] Weiher M, Herzig M, Tetzlaff R, Ascoli A, Mikolajick T and Slesazeck S 2019 *IEEE Trans. Circuits Syst.* I **66** 1–12